# Investigation of the Kinetic Mechanism of Cytidine 5′-Monophosphate *N*-Acetylneuraminic Acid Synthetase from *Haemophilus ducreyi* with New Insights on Rate-Limiting Steps from Product Inhibition Analysis†

Nicole M. Samuels, Bradford W. Gibson,* and Susan M. Miller*

*Department of Pharmaceutical Chemistry, University of California, San Francisco, California 94143-0446*

*Received February 5, 1999*

ABSTRACT: The presence of sialic acid as a component of cell surface lipooligosaccharides or capsular polysaccharides has been shown to be correlated with the virulence of a number of Gram-negative mucosal pathogens, including several *Haemophilus* and *Neisseria* spp. As part of our efforts to evaluate the role of sialic acid in the pathobiology of these organisms, we have initiated studies of the enzymes from *Haemophilus ducreyi* (the infectious agent of chancroid) responsible for the activation and attachment of sialic acid to the lipooligosaccharide. In this report, we describe results of an investigation of the steady-state kinetic mechanism of the activating enzyme, cytidine 5′-monophosphate *N*-acetylneuraminic acid (CMP-NeuAc) synthetase. Using a combination of initial velocity, product inhibition, and dead-end inhibition studies, the reaction is shown to be freely reversible and to proceed through an ordered bi-bi kinetic mechanism in which CTP binds first and CMP-NeuAc dissociates last. In addition, a detailed analysis of the kinetic expressions for the observable constants is presented showing how the variation in apparent product inhibition constants ($K_{ii}$) can be used to predict the rate-limiting step in $k_{cat}$, which appears to be dissociation of CMP-NeuAc in this enzyme. To our knowledge, this relationship has not been previously recognized.

Sialic acid [*N*-acetylneuraminic acid (NeuAc)[1]] is a nine-carbon acidic sugar whose presence on various surface glycoconjugates is known to modulate many cellular recognition processes (*1*, *2*). In many eukaryotes, sialic acid is widely distributed and appears on numerous cell surface glycoproteins and glycolipids. Besides there being known biological roles in cell−cell recognition and embryonic development, overexpression of sialic acid can occur in some tumors and is likely to contribute to their pathology (*3*, *4*). In contrast, sialic acid is found with much less frequency in prokaryotes, but nonetheless has been identified as a component of surface capsular polysaccharides and lipopolysaccharides (*4*−*6*). The appearance of sialic acid on bacterial glycoconjugates, for example, has been shown to correlate with the pathobiology and virulence of organisms that cause disease. Among pathogenic members of *Haemophilus* and *Neisseria* genera, sialic acid has been found to be linked to the terminal galactose of lactose, *N*-acetyllactosamine, and the trisaccharide Gal$\alpha$1→4Gal$\beta$1→4Glc ($P^K$ antigen) of some lipooligosaccharide (LOS) species (*5*, *7*, *8*). These same sialylated structures are also present as a component of human glycolipid antigens, suggesting that the functional role of LOS in some bacteria may be related to host mimicry, perhaps by serving as ligands for adhesion to and/or invasion of host tissues, or through the masking of bacterial cell surface antigens (*5*, *7*, *8*). In support of this hypothesis, the addition of sialic acid to the terminal epitopes of LOS has been demonstrated to confer serum resistance to *Neisseria gonorrheae* and to diminish the killing of *Neisseria meningitidis* by neutrophils (*9*). Given the importance of this acidic sugar in the modulation of virulence in pathogenic bacteria, the enzymes in the pathway for the synthesis, activation, and transfer of sialic acid to LOS represent potential targets for drug development.

The pathway for the biosynthesis of sialic acid in the *Haemophilus* and *Neisseria* genera has not yet been clearly established, but has been shown to involve condensation of *N*-acetylmannosamine with either PEP or pyruvate in other prokaryotes (*10*, *11*). However, the pathway for sialylation appears to be conserved in all organisms and involves two steps as shown in Figure 1. In the first step, CMP-NeuAc

† This work was supported by Grant AI 31254 (to B.W.G.) from the National Institutes of Health and by funds from the University AIDS Program (to B.W.G.). N.M.S. was partially supported by a Eugene-Cota Robles Fellowship and the Graduate Student Mentorship and Research Assistantship Program, both administered through the University of California, San Francisco.

* Questions regarding the kinetic analysis should be addressed to S.M.M. at School of Pharmacy S-926, 513 Parnassus Ave., University of California, San Francisco, CA 94143-0446. Telephone: (415) 476-7155. Fax: (415) 476-0688. E-mail: smiller@cgl.ucsf.edu. Send other questions to B.W.G. Telephone: (415) 476-5320. Fax: (415) 476-0688. E-mail: gibson@socrates.ucsf.edu.

[1] Abbreviations: BSA, bovine serum albumin; CMP-NeuAc, cytidine 5′-monophosphate *N*-acetylneuraminic acid; CTP, cytidine 5′-triphosphate; DTT, DL-dithiothreitol; G-1-P, α-D-glucose 1-phosphate; G-6-P, α-D-glucose 6-phosphate; HPLC, high-performance liquid chromatography; LOS, lipooligosaccharide; 2-*O*-Me-NeuAc, 2-*O*-methyl-$\beta$-*N*-acetylneuraminic acid; MOPS, 3-(*N*-morpholino)propanesulfonic acid; $NADP^+$, $\beta$-nicotinamide adenine dinucleotide phosphate; NADPH, reduced form of $\beta$-nicotinamide adenine dinucleotide phosphate; NeuAc, *N*-acetylneuraminic acid; PEP, phospho(enol)pyruvate; 6-P-GA, 6-phosphogluconic acid; $PP_i$, pyrophosphate; UDPG, uridine 5′-diphosphoglucose.

10.1021/bi990282j CCC: $18.00 
Published on Web 04/22/1999

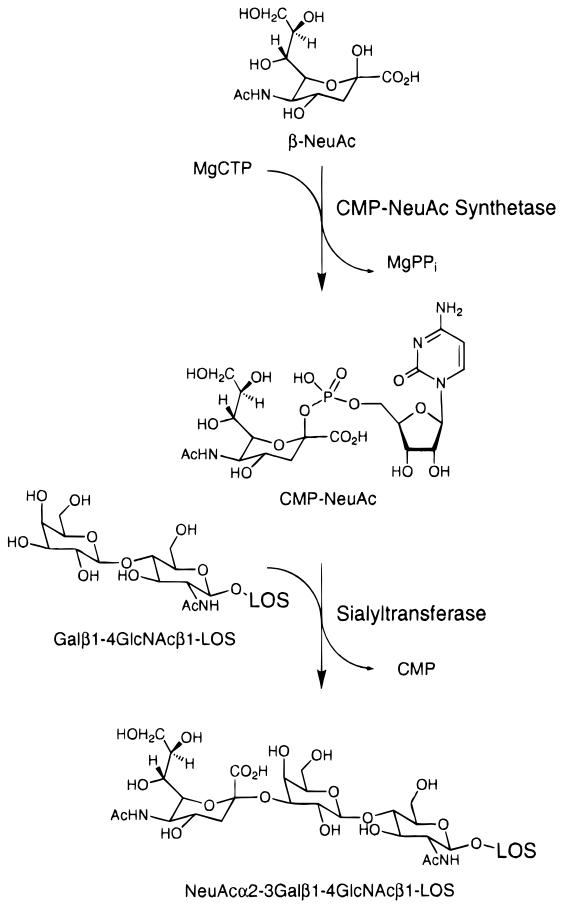


FIGURE 1: Biosynthetic pathway for sialylated LOS. CMP-NeuAc synthetase condenses free sialic acid with MgCTP, producing CMP-NeuAc and $MgPP_i$. CMP-NeuAc then serves as the substrate for a sialyltransferase, which catalyzes the transfer of the sialic acid to the nonreducing terminal *N*-acetyllactosamine of the LOS, in this case, at the 3′-position.

synthetase (EC 2.7.7.43) catalyzes the activation of the anomeric hydroxyl group in sialic acid by formation of an ester linkage in CMP-NeuAc, which then serves as the substrate for attachment of sialic acid to the LOS by one or more sialyltransferases. Recently, both sialyltransferase and CMP-NeuAc synthetase deletion mutants of *Haemophilus ducreyi* were constructed and shown by mass spectrometry and sugar composition analysis to be devoid of sialylated LOS glycoforms, although these sialic acid deficient mutants have not yet been assayed for changes in biological activity (*12*). In two cases where the biological consequences of introducing such a defect have been examined, that is, sialyltransferase deletion mutants of *N. gonorrheae* (*13*) and *N. meningitidis* (*14*), incorporation of sialic acid into the LOS was found to be critical for the conversion to and/or maintenance of a serum resistant phenotype. These studies strongly suggest that disruption of sialylation pathways in these organisms may provide an effective treatment for disease.

As indicated above, CMP-NeuAc is a common intermediate in both eukaryotic and prokaryotic organisms that display sialic acid on their cell surfaces, and a number of CMP-NeuAc synthetases have been isolated from both animal sources (*15*−*17*) and bacterial sources (*18*−*20*). Although several have been partially characterized, there has been no detailed kinetic analysis of any to provide a framework for rational drug design. We recently reported the cloning and expression of the CMP-NeuAc synthetase from *H. ducreyi* (*21*), the causative agent of chancroid (a genital ulcer disease), which has afforded large quantities of homogeneously pure enzyme for the initiation of basic biochemical studies. In one recent study, a conserved N-terminal lysine (Lys-19) was identified as a likely component of the CTP-binding domain (*22*). In the studies reported here, we have determined the steady-state kinetic mechanism of the *H. ducreyi* CMP-NeuAc synthetase using a combination of initial velocity kinetics, product inhibition, and dead-end inhibition studies, along with a detailed analysis of the kinetic expressions for the observable constants in the resulting ordered bi-bi mechanism. In this analysis, it is shown that the variation in the magnitude of apparent product inhibition constants can be used to predict rate-limiting steps in the reaction.

## MATERIALS AND METHODS

*Materials.* MOPS, $MgCl_2$, DTT, BSA, NeuAc, CTP, CMP-NeuAc, $PP_i$, UDPG, $NADP^+$, α-D-glucose 1,6-diphosphate, glucose-6-phosphate dehydrogenase, phosphoglucomutase, and uridine 5′-diphosphoglucose pyrophosphorylase were all purchased from Sigma Chemicals. 2-*O*-Me-NeuAc was purchased from GlycoTech.

*Preparation of CMP-NeuAc Synthetase*. The expression and purification of CMP-NeuAc synthetase from *H. ducreyi* were previously described (*21*). The enzyme was stored at 4 °C as an ammonium sulfate suspension. For assays in which the anion exchange HPLC method described below was used, stock solutions of CMP-NeuAc synthetase were made by dilution of the ammonium sulfate suspension with assay buffer containing 200 mM MOPS (pH 7.1), 200 mM NaCl, 20 mM $MgCl_2$, and 1 mg/mL BSA. However, for the enzyme-coupled fluorescence assay described below, the ammonium sulfate suspension of CMP-NeuAc synthetase was desalted prior to being used, by applying it to a Bio-Silect SEC-250 guard column (Bio-Rad; 50 mm × 7.8 mm) and eluting with 200 mM MOPS (pH 7.1) containing 200 mM NaCl. The total protein concentration of each enzyme preparation was quantitated using an extinction coefficient $\epsilon_{280}$ of 0.40 mL $mg^{-1}$ $cm^{-1}$ determined from the amino acid analysis of a sample of enzyme with a defined $A_{280}$.

*Anion Exchange HPLC Assay*. The rate of production of CMP-NeuAc was monitored by single-point measurements as previously described with slight modifications (*21*). Briefly, 90 μL of the premixed substrates is preincubated at 25 °C for 2 min prior to the addition of 10 μL of diluted CMP-NeuAc synthetase, resulting in the following final conditions: 200 mM MOPS (pH 7.1), 20 mM $MgCl_2$, 20 mM NaCl, and 0.1 mg/mL BSA. The final concentration of CMP-NeuAc synthetase was 0.71 nM for all experiments except for the dead-end inhibition study with NeuAc as the variable substrate, where it was 1.1 nM. For each enzyme concentration, limits for the duration of the initial linear phase were determined by measuring the initial velocity at multiple time points for the reactions where both substrates were either at the lowest or highest concentrations used in the full study, and also for the two reactions where one substrate was at its lowest and the other at its highest concentration. At appropriate times, reactions were terminated by addition of 20

Scheme 1: Enzyme-Coupled Fluorescence Assay for the Measurement of $PP_i$

$$\text{MgCTP} + \text{NeuAc} \xrightleftharpoons[\text{synthetase}]{\text{CMP-NeuAc}} \text{MgPP}_i + \text{CMP-NeuAc}$$

$$\text{MgPP}_i + \text{UDPG} \xrightleftharpoons[\text{pyrophosphorylase}]{\text{UDPG}} \text{UTP} + \text{G-1-P}$$

$$\text{G-1-P} \xrightleftharpoons[\text{glucomutase}]{\text{phospho-}} \text{G-6-P}$$

$$\text{G-6-P} + \text{NADP}^+ \xrightleftharpoons[\text{dehydrogenase}]{\text{G-6-P}} \text{6-P-GA} + \text{NADPH} + \text{H}^+$$

$\mu$L of 300 mM ammonium formate (pH 3.5), followed by immediate freezing on dry ice. The frozen reaction mixture was thawed just prior to being analyzed by anion exchange chromatography using a nucleotide analysis column (Vydac; 4.6 mm × 50 mm) with elution by a gradient of 35 to 500 mM ammonium formate (pH 3.5). The amount of CMP-NeuAc at each time point was determined by integration of its peak area measured at 280 nm using Mac Integrator I software (Rainin).

*Enzyme-Coupled Fluorescence Assay.* As an alternative assay for some of the product inhibition studies, CMP-NeuAc synthetase activity was monitored continuously by coupling the production of $PP_i$ to the reduction of $NADP^+$ via a series of three auxiliary enzymes (Scheme 1) (*23*). The coupling enzymes, their substrates, CTP, NeuAc, and CMP-NeuAc, as a product inhibitor, were premixed (360 $\mu$L) and preincubated at 25 °C for 2 min prior to the initiation of the reaction by addition of CMP-NeuAc synthetase (40 $\mu$L). Optimal conditions were determined to be 200 mM MOPS (pH 7.1), 1 mM UDPG, 0.5 mM $NADP^+$, 5 $\mu$M α-D-glucose 1,6-diphosphate (to activate phosphoglucomutase), 20 mM NaCl, 20 mM $MgCl_2$, 3 units/mL UDPG pyrophosphorylase (yeast), 8 units/mL phosphoglucomutase (rabbit muscle), 5 units/mL glucose-6-phosphate dehydrogenase (yeast), 0.1 mM DTT, 0.1 mg/mL BSA, and 70.2 nM CMP-NeuAc synthetase in a total volume of 400 $\mu$L. Prior to use, the ammonium sulfate suspension of phosphoglucomutase was exchanged into 200 mM MOPS (pH 7.1) containing 1 mM DTT, using a Microcon-10 microconcentrator (Amicon). The rate of NADPH formation was measured by following the increase in fluorescence ($\lambda_{ex}$ = 340 nm, with a slit width of 15 nm; $\lambda_{em}$ = 450 nm, with a slit width of 20 nm) using an LS 50B luminescence spectrometer (Perkin-Elmer). Under these conditions, the instrument response was found to be linear from 62 nM to 8 $\mu$M NADPH. Initial velocities were determined from the slope of the linear portion of the progress curve following the addition of CMP-NeuAc synthetase to the preincubated reaction mixture. The linear portion typically lasted from 40 to 150 s, and corresponded to less than 5% conversion of the substrate (at the lowest concentration) to product in each case.

*Substrate Initial Velocity Data.* The discontinuous anion exchange HPLC assay was used to obtain initial velocity data at varied concentrations of both substrates. The CTP concentration was varied from 12.5 to 100 $\mu$M as the concentration of NeuAc was varied from 62.5 $\mu$M to 1.0 mM to yield a 5 × 5 matrix. In each reaction, no more than 11% of the substrate in lowest concentration was converted to product. Each data point represents the mean of three separate trials.

*Product Inhibition Data.* The inhibition behavior of each product with respect to each substrate was determined by measuring initial velocities in the presence of a constant concentration of one substrate, while varying the concentration of the other substrate and the appropriate product, $PP_i$ or CMP-NeuAc. For studies of $PP_i$ as an inhibitor, production of CMP-NeuAc was assessed using the anion exchange HPLC assay. Conversely, for studies of CMP-NeuAc as an inhibitor, the generation of $PP_i$ was assessed indirectly by the enzyme-coupled assay (Scheme 1). Assay conditions were as described above with the exception of the addition of the chosen product inhibitor to the assay premix prior to the addition of CMP-NeuAc synthetase. Under these conditions, no more than 8% of the substrate at the lowest concentration was converted to product. Each data point represents the average of at least two separate trials.

*Dead-End Inhibition Data.* To examine the inhibition behavior of 2-*O*-Me-NeuAc with respect to each substrate, initial velocities were measured in the presence of a constant concentration of one substrate, while varying the concentrations of the other substrate and the inhibitor. For both types of reactions, production of CMP-NeuAc was assessed using the anion exchange HPLC assay. Conditions were as described above with the exception of the inclusion of 2-*O*-Me-NeuAc in the premix prior to the addition of CMP-NeuAc synthetase. Under these conditions, no more than 4% of the substrate at the lowest concentration was converted to product. Each data point represents the average of three separate trials.

*Data Analysis.* All experimental data were fit to rate equations by nonlinear regression analysis using KinetAsyst software (IntelliKinetics) employing the nomenclature of Cleland (*24*). Initial velocity data from the substrate kinetics were fit to the rate equation for a ternary complex mechanism (eq 1).

$$v = V_{max}[A][B]/(K_{ia}K_{mB} + K_{mA}[B] + K_{mB}[A] + [A][B]) \quad (1)$$

Data from the product and dead-end inhibition studies were fit to eqs 2−4 for competitive, uncompetitive, and noncompetitive inhibition, respectively.

$$v = V_{max}[S]/[K_{mS}(1 + [I]/K_{is}) + [S]] \quad (2)$$

$$v = V_{max}[S]/[K_{mS} + [S](1 + [I]/K_{ii})] \quad (3)$$

$$v = V_{max}[S]/[K_{mS}(1 + [I]/K_{is}) + [S](1 + [I]/K_{ii})] \quad (4)$$

where $v$ is the velocity, $V_{max}$ is the maximal velocity, $K_{ia}$ is the dissociation constant for the first substrate, $K_{mX}$ is the Michaelis constant for the designated substrate X, $K_{is}$ is the slope inhibition constant, $K_{ii}$ is the intercept inhibition constant, [I] is the inhibitor concentration, and S is the

Table 1: Kinetic Constants for CMP−NeuAc Synthetase

| substrate | $K_m$ ($\mu$M) | $k_{cat}$ ($s^{-1}$) | $K_{ia}$ ($\mu$M) |
|---|---|---|---|
| CTP | $10.6 \pm 1.2$ | $1.8 \pm 0.2$ | $44.6 \pm 6.8$[a] |
| NeuAc | $76.3 \pm 7.8$ | − | − |

[a] Based on the determination of the order of substrate addition below.

varied substrate in the inhibition experiments. Double-reciprocal plots of the data were created with Kaleidagraph (Synergy Software) using the kinetic constants obtained from the KinetAsyst analysis.

## RESULTS AND DISCUSSION

*Bisubstrate Initial Velocity Data.* As the first step in defining the kinetic mechanism, we have evaluated the pattern of variation in the initial velocity as a function of both substrates. Velocities were measured for a $5 \times 5$ matrix of CTP and NeuAc concentrations, and the data were displayed in double-reciprocal plots (Figure 2A,B) for the initial analysis of the pattern. The intersecting lines evident in the data indicate a mechanism with formation of a ternary enzyme−substrate complex (E·A·B) before the release of either product. However, the order of substrate binding and product release cannot be discerned from these data alone, since the presence of intersection points to the left of the *y*-axis in *both* plots is consistent with several random- and preferred-order mechanisms. Thus, the data were initially fit to a form of eq 1 in which the term $K_{ia}K_{mB}$ is simply designated $K_{ab}$ to obtain values for $k_{cat}$, $K_{mCTP}$, and $K_{mNeuAc}$, summarized in Table 1. The data do rule out obligatory ordered mechanisms (A followed by B) in which the first substrate (A) binds in a rapid equilibrium step, since this behavior gives an intersection of the lines in the $1/v$ versus 1/[B] plot *on* the *y*-axis.

*Product Inhibition Data.* To eliminate some of the possible pathways for substrate binding and product dissociation, we examined the ability of each product to inhibit the apparent steady-state constants for each substrate, apparent $k_{cat}$ and apparent $k_{cat}/K_m$, at fixed concentrations of the other substrate. Which constants are affected depends on three characteristics of the kinetic mechanism: (1) whether the chemical conversion is reversible, (2) the point(s) of product binding relative to the point of binding for each substrate, and (3) the concentration of the nonvaried substrate. To make accurate predictions of the expected patterns of inhibition, we first examined the reversibility of the chemical conversion. In previous studies of the CMP-NeuAc synthetase from *N. meningitidis* (*18*), no reversal of the reaction was detected when an indirect chemical assay was used to monitor the loss of CMP-NeuAc, or when a charcoal binding assay was used to monitor exchange of [$^{32}$P]$PP_i$ into CTP during normal turnover. We reexamined this question for the enzyme from *H. ducreyi* using our HPLC assay to directly monitor formation of CTP. Analysis of the time points from a reaction carried out under the same conditions that were used for the forward reaction, but with a higher concentration of CMP-NeuAc synthetase (56.8 nM), and 0.75 mM CMP-NeuAc and 3 mM $PP_i$, instead of CTP and NeuAc, clearly showed the time-dependent formation of CTP (data not shown). The estimated turnover number for this single set of conditions is 0.62 $s^{-1}$, only 3-fold lower than the $k_{cat}$ value determined for the forward reaction under the same conditions (1.8 $s^{-1}$, Table 1). Thus, the reaction appears to be freely reversible, and the product inhibition data should follow patterns for a chemically reversible reaction.

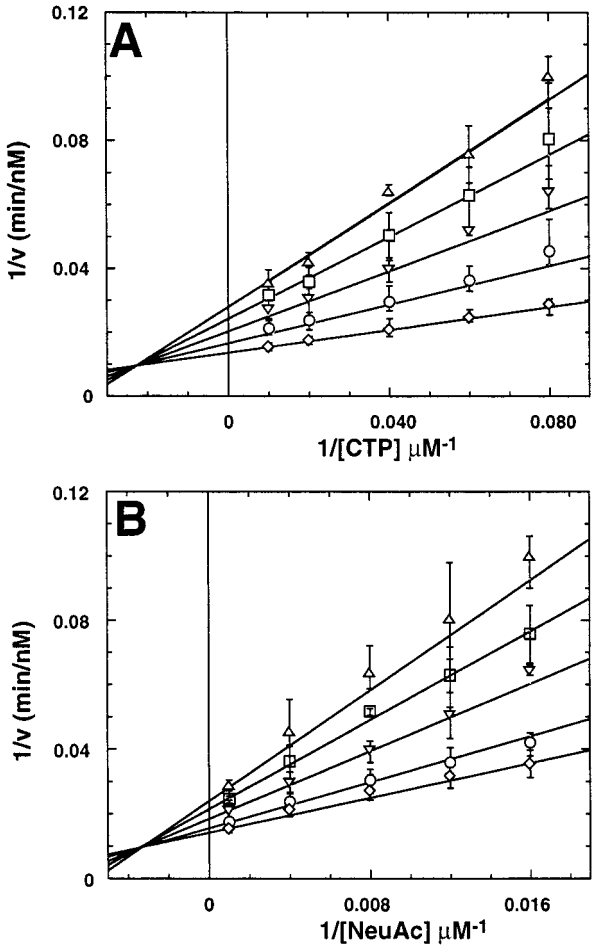


FIGURE 2: Initial velocity patterns for CMP-NeuAc synthetase. (A) Double-reciprocal plot with CTP as the varied substrate (12.5−100 $\mu$M) with fixed NeuAc concentrations of (△) 62.5 $\mu$M, (□) 83.3 $\mu$M, (▽) 125 $\mu$M, (○) 250 $\mu$M, and (◇) 1.0 mM. (B) Double-reciprocal plot with NeuAc as the varied substrate (62.5−1000 $\mu$M) with fixed CTP concentrations of (△) 12.5 $\mu$M, (□) 16.6 $\mu$M, (▽) 25 $\mu$M, (○) 50 $\mu$M, (◇) 100 $\mu$M.

As with all types of inhibitors, products are classified as competitive inhibitors if increasing concentrations decrease the apparent $k_{cat}/K_m$ for the varied substrate, uncompetitive if they decrease the apparent $k_{cat}$, and noncompetitive if they decrease both. The patterns are easily evaluated as increases in the slopes (apparent $K_m/k_{cat}$), the intercepts (apparent $1/k_{cat}$), or both, respectively, for lines in double-reciprocal plots of $1/v$ versus 1/[S] obtained at increasing concentrations of product (and a constant concentration of the second substrate). Double-reciprocal plots displaying the inhibition behavior of $PP_i$ and CMP-NeuAc versus both substrates are shown in Figures 3 and 4, respectively, and the associated patterns and inhibition constants derived from fits of the data to eqs 2−4 are summarized in Table 2. Comparison of the full set of patterns for all four substrate−product pairs with predicted sets of patterns at both saturating and subsaturating concentrations of the nonvaried substrate for a wide variety of mechanisms allows us to rule out random mechanisms and limit the possible obligatory-order mechanisms to the two shown in Scheme 2 (*25*). For the bi-bi ordered sequential

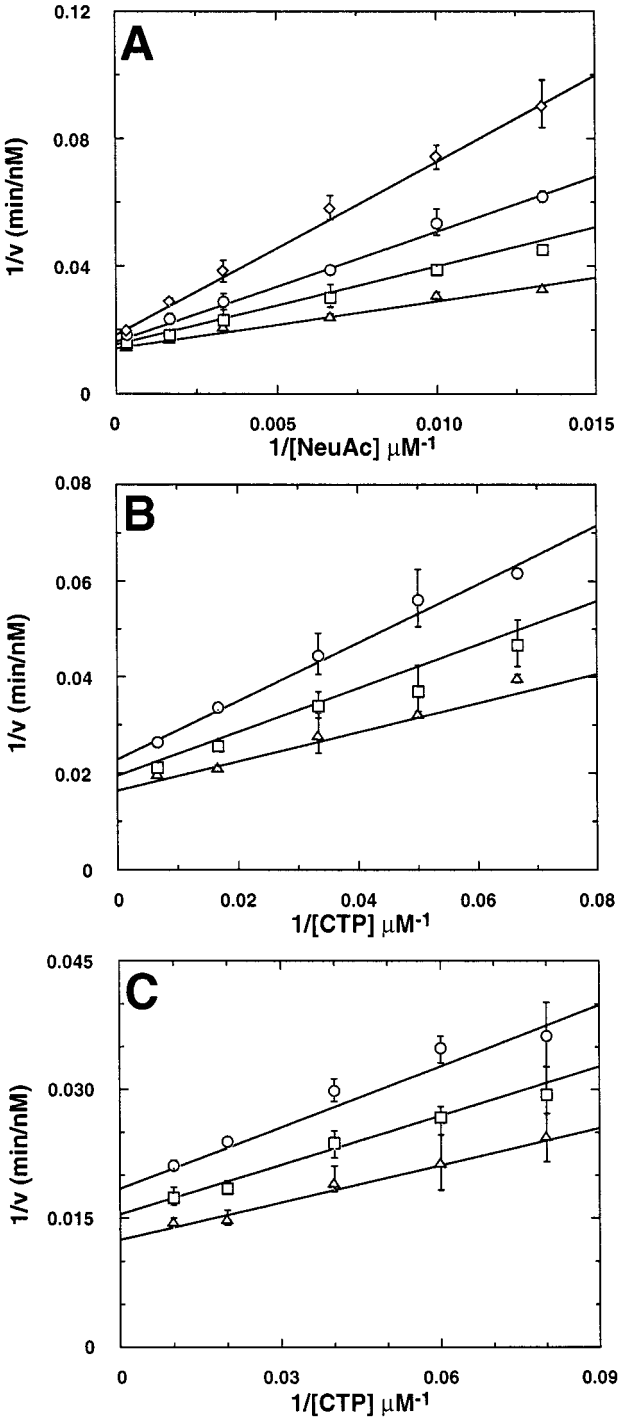


FIGURE 3: Product inhibition by $MgPP_i$. (A) Inhibition vs NeuAc as the varied substrate (0.075−3.0 mM), with fixed concentrations of (△) 0, (□) 0.5, (○) 1.0, and (◇) 2.0 mM $PP_i$. The CTP concentration was held constant at 100 $\mu$M. (B) Inhibition vs CTP as the varied substrate (15−150 $\mu$M), with fixed concentrations of (△) 0, (□) 0.5, and (○) 1.0 mM $PP_i$. The NeuAc concentration was held constant at 300 $\mu$M. (C) Inhibition vs CTP as the varied substrate (12.5−100 $\mu$M), with fixed concentrations of (△) 0, (□) 1.0, and (○) 2.0 mM $PP_i$. The NeuAc concentration was held constant at 2.0 mM. For all three plots, the lines were generated using constants obtained from fits of the data to eq 4 for noncompetitive inhibition. For comparison, the data in panel C were also fit to the uncompetitive model (eq 3); however, calculation of an $F_X$ value (*33*) from the variances for the two fits showed that inclusion of the extra variable in the noncompetitive model gave a better fit at the 99% confidence level.

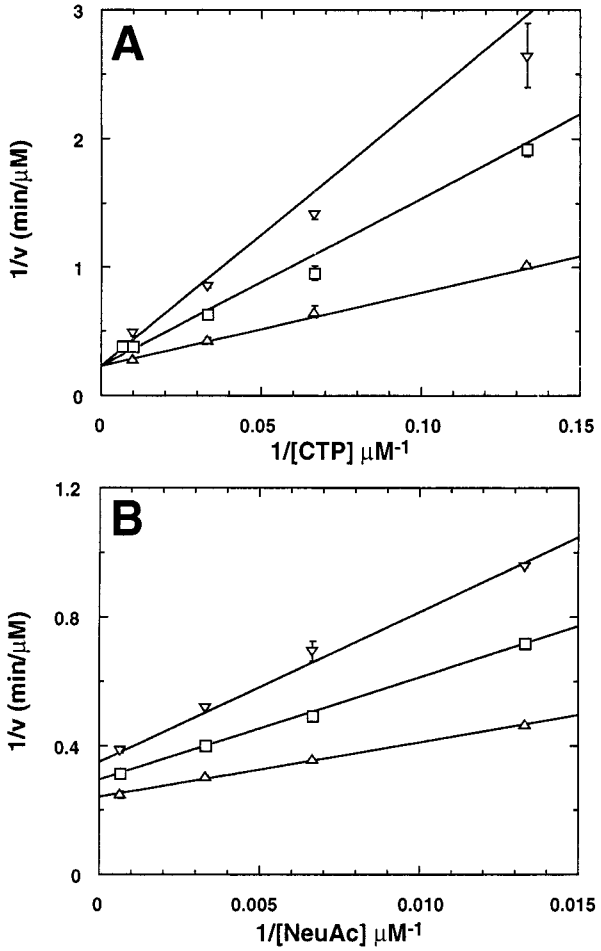


FIGURE 4: Product inhibition by CMP-NeuAc. (A) Inhibition vs CTP as the varied substrate (7.5−150 $\mu$M), with fixed concentrations of (△) 0, (□) 16, and (▽) 32 $\mu$M CMP-NeuAc. The NeuAc concentration was held constant at 1.5 mM. Lines were generated using constants obtained from a fit of the data to eq 2 for competitive inhibition. (B) Inhibition vs NeuAc as the varied substrate (0.075−1.5 mM), with fixed concentrations of (△) 0, (□) 16, and (▽) 32 $\mu$M CMP-NeuAc. The CTP concentration was held constant at 150 $\mu$M. Lines were generated using constants obtained from a fit of the data to eq 4 for noncompetitive inhibition.

mechanism depicted in Scheme 2A, competitive inhibition is observed for the first substrate−last product pair as they directly compete for binding to free enzyme. Thus, in this mechanism, CTP would be the first bound substrate and CMP-NeuAc the last dissociating product. In contrast, competitive inhibition is observed in the Iso Theorell-Chance mechanism in Scheme 2B for the second substrate−first product pair, since the interconversion of the binary enzyme−substrate and enzyme−product complexes is an equilibrium process limited only by the second-order rate constants for binding of the second substrate and first product. Thus, CTP and CMP-NeuAc would be the internal pair in this mechanism.

*Dead-End Inhibition Data.* The opposite order of substrate binding and product release predicted for the two mechanisms of Scheme 2 provides an avenue for distinction between the two using either direct binding assays or kinetic analysis of the pattern of inhibition by a structural homologue of one of the substrates (*26*). With our kinetic assays well in hand, we chose to examine the pattern of inhibition by the sialic acid analogue 2-*O*-Me-NeuAc, which has previously been shown to be a competitive inhibitor (with respect

Table 2: Product Inhibition Patterns and Constants for CMP-NeuAc Synthetase[a]

| inhibitor | varied substrate | constant substrate | pattern | $K_{is}$ | $K_{ii}$ |
|---|---|---|---|---|---|
| $PP_i$ | NeuAc | CTP (100 $\mu$M) | NC | 0.77 ± 0.10 mM | 6.70 ± 1.25 mM |
| $PP_i$ | CTP | NeuAc (300 $\mu$M) | NC | 1.00 ± 0.30 mM | 2.56 ± 0.60 mM |
| $PP_i$ | CTP | NeuAc (2.0 mM) | NC | 3.06 ± 1.07 mM | 4.20 ± 0.70 mM |
| CMP-NeuAc | NeuAc | CTP (150 $\mu$M) | NC | 18.8 ± 2.0 $\mu$M | 70.5 ± 5.6 $\mu$M |
| CMP-NeuAc | CTP | NeuAc (1.5 mM) | C | 12.5 ± 1.7 $\mu$M | – |

[a] Experimental conditions are as described in Materials and Methods. The errors reported for the inhibition constants are the standard errors for the fits to the corresponding rate equations. C represents competitive, and NC represents noncompetitive. $K_{ii}$ and $K_{is}$ are intercept and slope inhibition constants, respectively.

Scheme 2: Potential Kinetic Mechanisms for CMP-NeuAc Synthetase with (A) the Ordered Bi-Bi Mechanism and (B) the Iso Theorell-Chance Mechanism[a]

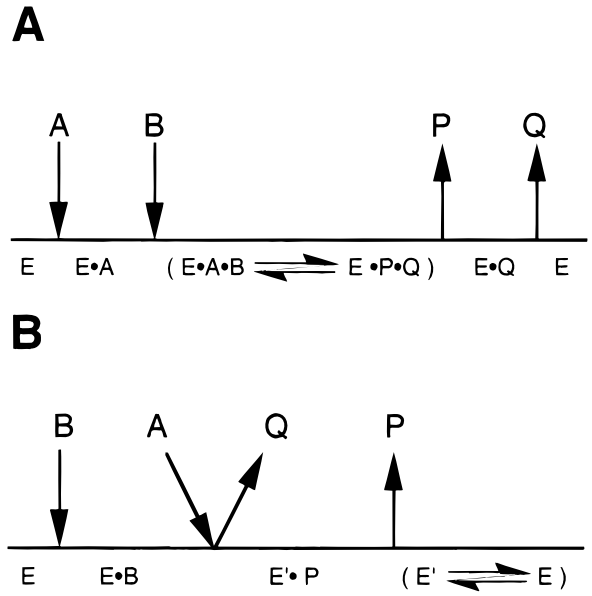


[a] A is CTP. B is NeuAc. P is $PP_i$. Q is CMP-NeuAc.

to NeuAc) of the CMP-NeuAc synthetase from *Escherichia coli* [$K_i$ of 2.5 mM (*27*)]. Clearly, competitive inhibition with respect to NeuAc is expected for both mechanisms. The distinction lies in the expected pattern with respect to CTP. Binding of the inhibitor after CTP (to E·CTP) in the bi-bi mechanism will affect only the apparent $k_{cat}$, thereby giving an uncompetitive pattern, while binding before CTP (to E) provides a reversible link at subsaturating NeuAc concentrations, thereby giving a noncompetitive pattern for the Iso Theorell-Chance mechanism. As shown in Figure 5A, 2-*O*-Me-NeuAc does indeed exhibit a competitive inhibition pattern with respect to NeuAc, confirming that they bind to the same enzyme form. The fit of the initial velocity data to the equation for competitive inhibition (eq 2) yields a dissociation constant $K_{is}$ of 64.5 ± 15.5 $\mu$M. Conversely, when NeuAc is held constant, increasing concentrations of 2-*O*-Me-NeuAc give rise to an uncompetitive inhibition pattern versus CTP (Figure 5B), consistent with the downstream binding of 2-*O*-Me-NeuAc relative to CTP predicted for the bi-bi mechanism.

*Relative Magnitudes of Some Microscopic Constants from Inhibition Data.* The minimal kinetic mechanism for the *H. ducreyi* CMP-NeuAc synthetase consistent with the combined results is shown in Scheme 3, together with expressions for several of the observed kinetic constants in terms of the individual rate constants and equilibrium constants within this scheme. Because of the complexity of the expressions,

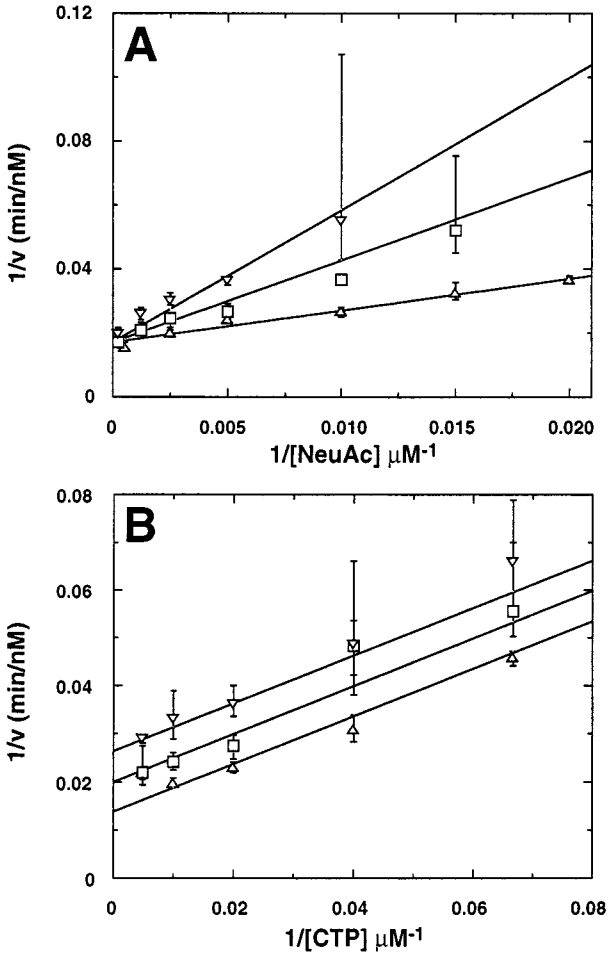


FIGURE 5: Inhibition of CMP-NeuAc synthetase by 2-*O*-Me-NeuAc. (A) Double-reciprocal plot with NeuAc as the varied substrate (50−4000 $\mu$M) at fixed 2-*O*-Me-NeuAc concentrations of (△) 0, (□) 100, and (▽) 200 $\mu$M. The CTP concentration was held constant at 300 $\mu$M. The $K_i$ was generated from the fit of the data to eq 2 for competitive inhibition. (B) Double-reciprocal plot with CTP as the varied substrate (15−200 $\mu$M) at fixed 2-*O*-Me-NeuAc concentrations of (△) 0, (□) 125, and (▽) 250 $\mu$M. The NeuAc concentration was held constant at 300 $\mu$M. The data were fit to eq 3 for uncompetitive inhibition.

the initial velocity data alone provide little information regarding rate-limiting steps or the magnitudes of internal equilibrium steps. However, an examination of the expressions for the inhibition constants obtained in this study shows that analysis of the magnitudes and trends in these values provides some insight into the relative magnitudes of a few of the microscopic constants in the mechanism.

Consider first the expressions for the apparent $K_{iiPP_i}$ constants as a function of the nonvaried substrate concentration (Scheme 3). In each expression, the right-hand factor is the limiting value that would be observed when both

Scheme 3: Minimal Kinetic Mechanism for CMP-NeuAc Synthetase and Expressions for Observed Kinetic Constants

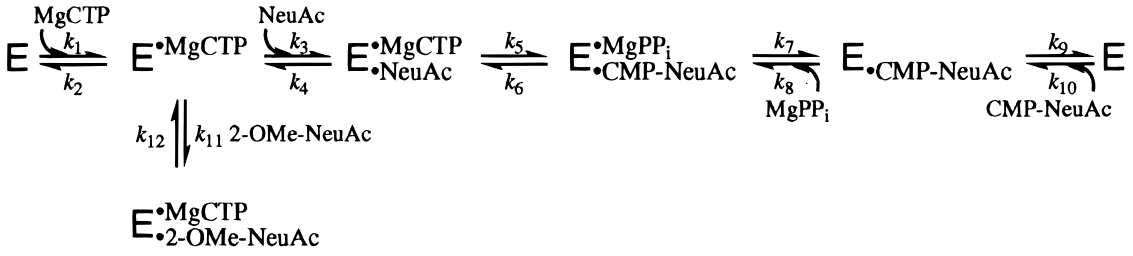


$$K_{mCTP} = \frac{k_{cat}}{k_1} \qquad K_{mNeuAc} = \frac{k_4(k_6 + k_7)k_9 + k_5k_7k_9}{k_3[k_9(k_6 + k_7) + k_5k_7 + k_5k_9]} \qquad k_{cat} = \frac{k_5k_7k_9}{k_9(k_6 + k_7) + k_5k_7 + k_5k_9}$$

$$K_{iCTP} = \frac{k_2}{k_1} \qquad K_{is2\text{-}OMe\text{-}NeuAc} = \frac{k_{12}}{k_{11}} \qquad K_{isCMP\text{-}NeuAc\ (vs\ CTP)} = \frac{k_9}{k_{10}}$$

$$K_{iiPPi\ (vs\ NeuAc)} = \left(\frac{k_1CTP + k_{cat}}{k_1CTP}\right)\left(\frac{k_5k_9K_{dPPi}}{k_{cat}(k_5 + k_6)}\right) \qquad K_{iiPPi\ (vs\ CTP)} = \left(\frac{NeuAc + K_{mNeuAc}}{NeuAc + \frac{K_{dNeuAc}}{(1 + K_{eq})}}\right)\left(\frac{k_5k_9K_{dPPi}}{k_{cat}(k_5 + k_6)}\right)$$

$$K_{dPPi} = \frac{k_7}{k_8} \qquad K_{dNeuAc} = \frac{k_4}{k_3} \qquad K_{eq} = \frac{k_5}{k_6}$$

Table 3: Simplified Expressions for $k_{cat}$ and $K_{mNeuAc}$ for Different Rate-Limiting Steps in $k_{cat}$

| | $k_{cat}$ = | $K_{mNeuAc}$ = |
|---|---|---|
| all steps similar | $\frac{k_5k_7k_9}{k_9(k_6 + k_7) + k_5k_7 + k_5k_9}$ | $\frac{k_4(k_6 + k_7)k_9 + k_5k_7k_9}{k_3[k_9(k_6 + k_7) + k_5k_7 + k_5k_9]}$ |
| $k_5 << k_7, k_9$ | $\frac{k_5k_7}{k_6 + k_7}$ | $K_{dNeuAc} + \frac{k_5k_7}{k_3(k_6 + k_7)}$ |
| $k_7 << k_5, k_9$ | $\frac{K_{eq}k_7}{(1 + K_{eq})}$ | $\frac{K_{dNeuAc}}{(1 + K_{eq})}$ |
| $k_9 << k_5, k_7$ | $k_9$ | $\frac{k_9\{k_4[(k_6/k_7) + 1] + k_5\}}{k_3\,k_5}$ |

substrates are fully saturating, while the other factor describes the expected trend in the apparent value as the concentration of the fixed substrate is varied. Comparison of these latter factors shows that while $K_{iiPP_i}$ versus NeuAc will always decrease to the limiting value as the CTP concentration increases, $K_{iiPPi}$ versus CTP may decrease or increase to the limiting value as the NeuAc concentration increases, depending on the relative magnitudes of $K_{mNeuAc}$ and the term $K_{dNeuAc}/(1 + K_{eq})$. If $K_{mNeuAc}$ is smaller, $K_{iiPP_i}$ increases as the NeuAc concentration increases; if $K_{mNeuAc}$ is larger, $K_{iiPP_i}$ decreases as the NeuAc concentration increases, and if the terms are equal, $K_{iiPP_i}$ is independent of NeuAc concentration. By substituting the values for $k_{cat}$, $k_1$ ($=k_{cat}/K_{mCTP}$, Scheme 3), and CTP concentration into the expression for the apparent $K_{iiPP_i}$ versus NeuAc shown in Scheme 3, we estimate the limiting value for $K_{iiPP_i}$ to be 6.1 ± 1.7 mM. Comparison of this value with the data for $K_{iiPP_i}$ versus CTP in Table 2 shows an increase in the apparent value toward this limiting value as the NeuAc concentration increases, indicating that $K_{mNeuAc} < K_{dNeuAc}/(1 + K_{eq})$ and likewise that $K_{mNeuAc} < K_{dNeuAc}$. Analysis of the expression for $K_{mNeuAc}$ in Table 3 indicates that the direction of this relationship is directly dependent on which step is rate-limiting in $k_{cat}$. When the chemical step, $k_5$, is rate-limiting, $K_{mNeuAc} = K_{dNeuAc}$, and when dissociation of $PP_i$, $k_7$, is rate-limiting, $K_{mNeuAc} = K_{dNeuAc}/(1 + K_{eq})$. The only condition under which $K_{mNeuAc}$ can be less than $K_{dNeuAc}/(1 + K_{eq})$ is when $k_9$ is significantly rate-limiting. In addition, the observation of $K_{mNeuAc} < K_{dNeuAc}$ also indicates that the rate constant for dissociation of NeuAc, $k_4$, must be greater than that of the rate-limiting dissociation of product (*28*). *Thus, the trend observed in the $K_{iiPP_i}$ data strongly suggests that dissociation of CMP-NeuAc,*

*$k_9$, is the major rate-limiting step in this reaction and that $k_4 > k_9$.*

Another analysis supporting the conclusion that $k_9$ is significantly rate-limiting comes from a comparison of the rate constants for association and dissociation of CTP ($k_1$ and $k_2$, respectively) with minimal estimates of the values for association and dissociation of CMP-NeuAc ($k_{10}$ and $k_9$, respectively) derived from the observed equilibrium dissociation constant $K_{isCMP-NeuAc}$ (Scheme 3 and Table 2). From the expressions for $K_{mCTP}$ and $K_{iCTP}$ (which is extracted from the initial velocity data as $K_{ia}$ in eq 1), we calculate values for $k_1$ and $k_2$ of $1.7 \times 10^5$ $M^{-1}$ $s^{-1}$ and 7.6 $s^{-1}$, respectively. By comparison, if dissociation of CMP-NeuAc is completely rate-limiting in $k_{cat}$, that is $k_9 \approx 1.8$ $s^{-1}$, the minimal value for the association rate constant for CMP-NeuAc, $k_{10}$, is $1.4 \times 10^5$ $M^{-1}$ $s^{-1}$, a value remarkably close to that of $k_1$ and consistent with the substantial retention of the CTP structure in CMP-NeuAc. If $k_9$ were not at least partially rate-limiting, the values for both $k_9$ and $k_{10}$ would be at least 10-fold larger than these minimal values and, hence, larger than the rate constants for CTP binding, which seems less likely considering the increased bulk and number of potential hydrogen bonding interactions in the structure of CMP-NeuAc compared with those of CTP. Thus, the data provide a self-consistent indication that the dissociation of CMP-NeuAc is significantly rate-limiting in the forward reaction.

One additional piece of information that falls out of the product and dead-end inhibition data is that the magnitude of $K_{dNeuAc}$ is somewhat larger than the corresponding dissociation constant measured for the highly similar analogue 2-*O*-Me-NeuAc. Rearrangement of the expression for $K_{iiPP_i}$ versus CTP, and substitution of the limiting and measured values, yields the relationship $K_{dNeuAc}/K_{mNeuAc} = (1 + K_{eq})(10 \pm 6)$, which translates into $K_{dNeuAc}/K_{is2-O-Me-NeuAc} \approx (1 + K_{eq})(10 \pm 6)$ since $K_{mNeuAc}$ ($\sim$76 $\mu$M) $\approx$ $K_{is2-O-Me-NeuAc}$ ($\sim$64 $\mu$M). This indicates that the analogue binds at least ($10 \pm 6$)-fold more tightly than the substrate to the E·CTP complex, but the disparity could be substantially larger if the internal equilibrium of the chemical conversion step lies far to the right ($K_{eq} \geq 1$). Thus, it is interesting to consider what factors could enhance the binding of 2-*O*-Me-NeuAc versus NeuAc and to what extent. With regard to the structure of $\beta$-NeuAc in Figure 1, the only difference between it and 2-*O*-Me-NeuAc is the replacement of the hydrogen on the reactive anomeric oxygen by a methyl group. Three properties change as a result of this replacement: (1) the steric bulk at the reactive oxygen, (2) the solvation of OH versus OR, and (3) the ability to anomerize. Because it increases the steric bulk at the reactive center, the methyl group might be expected to decrease the binding affinity of the analogue rather than increasing it. However, if the active site can accommodate the extra bulk, the methyl group could enhance the affinity to a small extent since the OMe should require less desolvation than the OH group upon binding to the active site; desolvation of the OH would be expected since this group, in its deprotonated state, acts as a nucleophile in the reaction.[2] The third property altered by the presence of the methyl group is the stability of the $\beta$-configuration at the anomeric carbon. The 2-*O*-Me analogue is a stable $\beta$-glycoside, while NeuAc is a hemiketal that can undergo anomerization. Once again, however, this should only increase $K_{dNeuAc}$ versus $K_{is2-O-Me-NeuAc}$ by a minor amount, since at equilibrium approximately 93% of the NeuAc is present as the correct $\beta$-anomer (*29*). With only these two small factors expected to enhance the affinity of the analogue versus the substrate for the enzyme, it seems unlikely that the affinities for the two would differ by much more than 1 order of magnitude. This then leads to the prediction that the internal equilibrium constant for the chemical conversion step, $K_{eq}$, does not deviate too far from a value of 1, a common result found for many enzymes.

*Relationship with Other CMP-NeuAc Synthetases.* Having established a mechanism for the *H. ducreyi* CMP-NeuAc synthetase, one would like to know whether this mechanism is conserved throughout the larger CMP-NeuAc synthetase family and whether specific members of this family can be considered appropriate targets for drug design. Since the biosynthetic pathways leading to the synthesis of sialic acid-containing glycoconjugates in both prokaryotes and eukaryotes require the formation of CMP-NeuAc as the activated sugar donor, the feasibility of developing inhibitors that selectively target, for example, CMP-NeuAc synthetase from pathogenic bacteria over the human host's enzyme will require the existence of some notable differences in their properties. Despite the limited information regarding the kinetic and mechanistic properties of this enzyme family, at least a couple of comparisons can be made. Examination of alignments of the eight reported gene sequences to date reveals two subgroups, proteins approximately 225 amino acids in length, including those from pathogenic strains of *Haemophilus* and *Neisseria* spp. and proteins that are more than 400 amino acids in length, including those from *E. coli*, *Streptococcus agalactiae*, *Campylobacter coli* (*21*), and, perhaps most importantly, the first full mammalian sequence to be reported from mice (*30*). Complete conservation of several residues in the whole family, including a lysine (K19) identified in the CTP binding site of the *H. ducreyi* enzyme (*22*), suggests similar chemical mechanisms of catalysis in the two groups. However, the observation of micromolar $K_m$ values for the smaller enzymes (this work and refs *18* and *21*) compared with millimolar values reported for some of the larger enzymes (*20*, *31*, *32*), as well as the 64 $\mu$M $K_{is2-O-Me-NeuAc}$ value reported here for the *H. ducreyi* enzyme versus a value of 2.5 mM for the *E. coli* enzyme (*27*), suggests that there may be exploitable kinetic differences between these groups of enzymes. In addition, the cellular location of the bacterial versus the mammalian enzymes may provide a further selective advantage, since the bacterial enzymes are cytoplasmic, while the mammalian enzymes are located in the nucleus (*30*). These observations, together with the kinetic picture developed in this work, provide a framework for further investigation of this group of enzymes.

[2] Although this has not been shown explicitly for the *H. ducreyi* enzyme, retention of the $^{18}O$ label in the anomeric hydroxyl upon conversion of 2-[$^{18}O$]-$\beta$-NeuAc to CMP-NeuAc has been demonstrated using the *E. coli* enzyme (*29*).

## ACKNOWLEDGMENT

We thank Dr. Judith Klinman and Dr. Michael V. Tullius for helpful discussions.

## REFERENCES


1. Rosenberg, A. (1995) *Biology of Sialic Acids*, Plenum Press, New York.
2. Kelm, S., and Schauer, R. (1997) *Int. Rev. Cytol. 175*, 137−240.
3. Kern, W. F., Spier, C. M., Miller, T. P., and Grogan, T. M. (1993) *Leuk. Lymphoma 12*, 1−10.
4. Reglero, A., Rodriguez-Aparicio, L. B., and Luengo, J. M. (1993) *Int. J. Biochem. 25*, 1517−1527.
5. Moran, A. P., Prendergast, M. M., and Appelmelk, B. J. (1996) *FEMS Immunol. Med. Microbiol. 16*, 105−115.
6. Bitter-Suermann, D. (1993) in *Polysialic Acid: From Microbes to Man* (Roth, J., Rutishauser, U., and Troy, F. A., Eds.) pp 11−24, Birkhäuser Verlag, Basel, Switzerland.
7. Mandrell, R. E., and Apicella, M. A. (1993) *Immunobiology 187*, 382−402.
8. Preston, A., Mandrell, R. E., Gibson, B. W., and Apicella, M. A. (1996) *Crit. Rev. Microbiol. 22*, 139−180.
9. Smith, H., Parsons, N. J., and Cole, J. A. (1995) *Microb. Pathog. 19*, 365−377.
10. Ferrero, M. A., Reglero, A., Fernandez-Lopez, M., Ordas, R., and Rodriguez-Aparicio, L. B. (1996) *Biochem. J. 317*, 157−165.
11. Vann, W. F., Tavarez, J. J., Crowley, J., Vimr, E., and Silver, R. P. (1997) *Glycobiology 7*, 697−701.
12. Bozue, J. L., Tullius, M. V., Wang, J., Gibson, B. W., and Musson, R. S. J. (1999) *J. Biol. Chem. 274*, 4106−4114.
13. Bramley, J., Demarco de Hormaeche, R., Constantinidou, C., Nassif, X., Parsons, N., Jones, P., Smith, H., and Cole, J. (1995) *Microb. Pathog. 18*, 187−195.
14. Kahler, C. M., Martin, L. E., Shih, G. C., Rahman, M. M., Carlson, R. W., and Stephens, D. S. (1998) *Infect. Immun. 66*, 5939−5947.
15. Schmelter, T., Ivanov, S., Wember, M., Stangier, P., Thiem, J., and Schauer, R. (1993) *Biol. Chem. Hoppe-Seyler 374*, 337−342.
16. Schauer, R., Haverkamp, J., and Ehrlich, K. (1980) *Hoppe-Seyler's Z. Physiol. Chem. 361*, 641−648.
17. Rodriguez-Aparicio, L. B., Luengo, J. M., Gonzalez-Clemente, C., and Reglero, A. (1992) *J. Biol. Chem. 267*, 9257−9263.
18. Warren, L., and Blacklow, R. S. (1962) *J. Biol. Chem. 237*, 3527−3534.
19. Vann, W. F., Silver, R. P., Abeijon, C., Chang, K., Aaronson, W., Sutton, A., Finn, C. W., Linder, W., and Kotsatos, M. (1987) *J. Biol. Chem. 262*, 17556−17562.
20. Haft, R. F., and Wessels, M. R. (1994) *J. Bacteriol. 176*, 7372−7374.
21. Tullius, M. V., Munson, R. S., Wang, J., and Gibson, B. W. (1996) *J. Biol. Chem. 271*, 15373−15380.
22. Tullius, M. V., Vann, W. F., and Gibson, B. W. (1999) *Protein Sci. 8*, 666−675.
23. Passonneau, J. V. (1993) *Enzymatic Analysis: A Practical Guide*, Humana Press, Totowa, NJ.
24. Cleland, W. W. (1963) *Biochim. Biophys. Acta 67*, 104−137.
25. Segel, I. H. (1975) *Enzyme Kinetics: Behavior and Analysis of Rapid Equilibrium and Steady-State Enzyme Systems*, Wiley, New York.
26. Fromm, H. J. (1995) *Methods Enzymol. 249*, 123−143.
27. Schmid, W., Christian, R., and Zbiral, E. (1988) *Tetrahedron Lett. 29*, 3643−3646.
28. Klinman, J. P., and Matthews, R. G. (1985) *J. Am. Chem. Soc. 107*, 1058−1060.
29. Ambrose, M. G., Freese, S. J., Reinhold, M. S., Warner, T. G., and Vann, W. F. (1992) *Biochemistry 31*, 775−780.
30. Münster, A. K., Eckhardt, M., Potvin, B., Muhlenhoff, M., Stanley, P., and Gerardy-Schahn, R. (1998) *Proc. Natl. Acad. Sci. U.S.A. 95*, 9140−9145.
31. Vann, W. F., Zapata, G., Roberts, I. S., Boulnois, G., and Silver, R. P. (1993) in *Polysialic Acid: From Microbes to Man* (Roth, J., Rutishauser, U., and Troy, F. A., Eds.) pp 125−136, Birkhäuser Verlag, Basel, Switzerland.
32. Liu, J. L.-C., Shen, G.-J., Ichikawa, Y., Rutan, J. F., Zapata, G., Vann, W. F., and Wong, C.-H. (1992) *J. Am. Chem. Soc. 114*, 3901−3910.
33. Bevington, P. R. (1969) *Data Reduction and Error Analysis for the Physical Sciences*, McGraw-Hill, Inc., New York.


BI990282J